Flood Risk and Flow Variability Assessment at the Railway Drainage Structures: A Case of the Ethio – Djibouti Railway Line, Ethiopia

Habeeb Solihu*[1]

Belete Berhanu Kidanewold[1]

Abdulwasiu Abdulkadir[4]

Abstract

Awash River Subbasin is one of the major river flood-prone areas in Ethiopia where the most significant part of the railway section is constructed. There is tendency of this railway line being affected by flooding. The study performed the flood risk analysis and flow variability at some selected drainage structures within Sebeta and Adama Section of this line. The climate and observed flow data were sourced from the National Meteorological Agency of Ethiopia and the Ministry of Water, Irrigation and Energy of Ethiopia respectively, and used for hydrological model parametrization, calibration, and validation. DMC, Linear Regression, and Thiessen Polygon were used for climate data consistency check, filling of missing data, and estimation of areal data respectively. The rainfall-runoff was simulated with an HEC-HMS hydrological model using a 20years (2000 – 2019) rainfall data. The model calibration and validation results using NSE, PBIAS, and R^2, were found within the statistically acceptable range for the surface runoff simulation. This study developed Rainfall Intensity – Duration Frequency Curve for the selected catchment as an input for the flood frequency analysis in the model. The coefficient of variance was estimated to select the flood discharge structures with the flow variabilities. The flood risk was assessed by comparing the modeled and the as built designed Q_{100} (m^3/s) extracted from the design documents. About 46% of the drainage structures are found prone to flooding at a $T_{100years}$. This study recommends the use of the methodological procedure adopted in this study for other section of this line by other researchers.

Key Words: Flood Risk; Flow Variability; Hydrological Model; Railway; Risk Assessment

[1]School of Civil Engineering and Environmental Engineering, Addis Institute of Technology, Addis Ababa University, Addis Ababa, Ethiopia, [2]Department of Civil Engineering, Faculty of Engineering, University of Abuja, Abuja, Nigeria, [3]Department of Civil Engineering, Faculty of Engineering and Technology, Kwara State University, Malete, Kwara State, Nigeria, [4]Institute of Technology, Kwara State Polytechnic, Ilorin, Kwara State, Nigeria

*Corresponding Author's e-mail: solihu.habeeb@aait.edu.et

Received on December 10, 2021/Accepted on August 21, 2022

Ghana Journal of Geography Vol. 14 (2), 2022 pages 175-208

Doi: https://dx.doi.org/10.4314/gjg.v14i3.7

Introduction

Rail transportation is a key enabler of economic growth worldwide and it consists of two main asset classes of infrastructure and rolling stock (Dinmohammadi et al., 2016). Reinforced concrete bridges are the backbone of bridge structures (Liu et al., 2020) and the effects of water must be properly managed during the different phases of the lifecycle of these infrastructures such as a railway to avoid closure or even partial destruction (Sañudo et al., 2019). To establish the actual bridge behavior and allowing for the effects of the possible imperfections or damages of the structural members, the spatial computational models should be used for global analyses of steel railway bridges (Vičan et al., 2016).

Awash River Subbasin is one of the major river flood-prone areas in Ethiopia where the most significant part of the railway section is constructed. There is tendency of this railway line being affected by flooding. Thus, this is the rationale for this study. Therefore, to maintain the socio-economic importance of this line connecting the Ethiopia and the Djibouti together, the study performed the flood risk analysis and flow variability at some selected drainage structures within Sebeta and Adama Section of this line. The study investigated the flow variability impacts on flooding risk at some selected flood discharge structures within the Sebeta – Adama Section of Ethio – Djibouti Railway line.

The study developed a rainfall-runoff model for the selected section (Sebeta – Adama of Ethio – Djibouti Railway Line) to investigate flow variability; an Intensity Duration Frequency curve was developed to estimate the design rainfall as an input to the HEC-HMS model to estimate the peak flows. In addition, the flood risk associated with each peak flow were estimated. This is so important because drainage structures (bridges and culverts) are the major components of a traffic

system whereby any damage to any of its components has the potential of causing loss of lives and properties (Feng et al., 2021). This can affect the economy of the state either directly or indirectly. From Table 1 and Figure 1, there is a rapid increase in urbanization as the percentage area occupied by built-up area class increased from 1.9% to 9.6% from 2016 to 2020 respectively. Although the preponderate LandCover class is cropland with 81.6% and 65.4% for 2016 and 2020 respectively. This implies the major activity in the study area is Agriculture; however, there was a decrease of about 22% in the agricultural activities in the LandUse between 2016 and 2020.

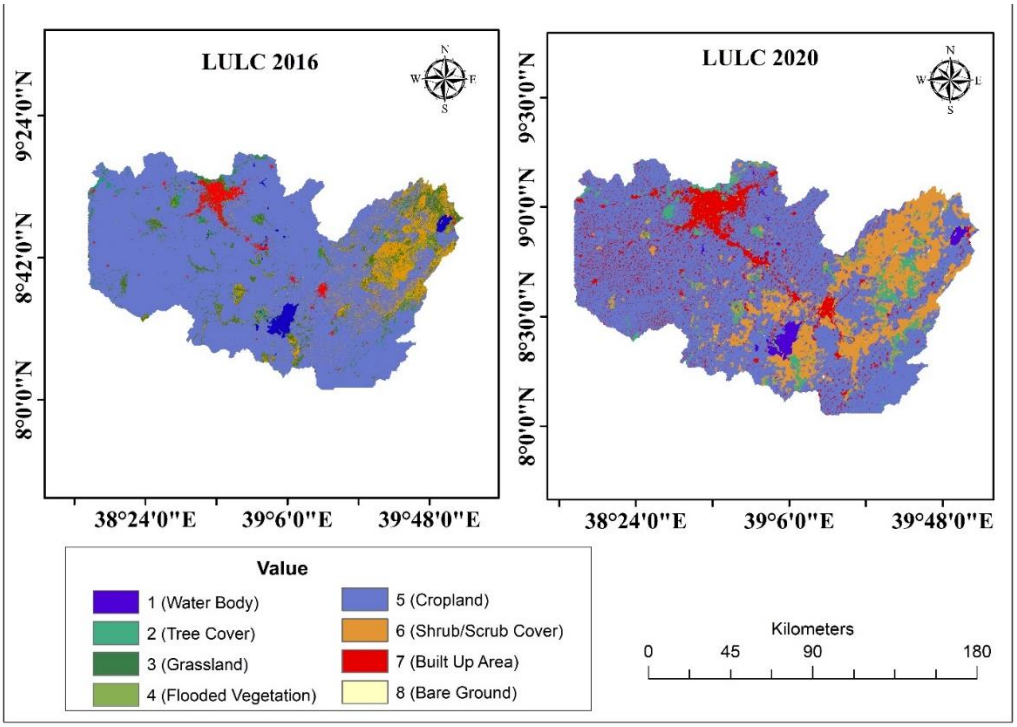


Figure 1: LandUse LandCover Changes between Years 2016 and 2020

Table 1: LandUse LandCover Classifications between 2016 and 2020

LULC Class	2016		2020		%Change
	Area_km	Area (%)	Area_km	Area (%)	
Bare Areas	11.5	0.1	16.7	0.1	0.0
Built Up Areas	322.2	1.9	1641.7	9.6	7.7
Croplands	13894.3	81.6	11131.4	65.4	-16.2
Flooded Vegetation	16.6	0.1	21.4	0.1	0.0
Grasslands	1021.2	6.0	35.5	0.2	-5.8
Shrubs Cover Areas	1293.7	7.6	3092.1	18.2	10.6
Tree Cover Areas	241.3	1.4	837.6	4.9	3.5
Water Body	229.6	1.3	253.8	1.5	0.2
Total	**17030.4**	**100.0**	**17030.4**	**100.0**	

Literature Review

Railways remain the safest and the most economical ground transport means for commuters (An et al., 2013; Sekasi & Solihu, 2021). Railway tracks, rail switches, other engineering structures such as bridges, tunnels, and associated infrastructure of stations, which includes platforms, security, and safety devices (Hofreiter et al., 2013), form railway infrastructure. Failure of these critical infrastructures for conveying people and freight services must be controlled as much as possible to maintain safety and to limit economic losses (Lagadec et al., 2018).

(Wardhana & Hadipriono, 2003) reported that there were 500 cases of bridge structure failures between 1989 and 2000 in the United States. They further contend that the main cause of the failures was floods and the scouring process. In addition, on July 9, 1981, during a debris flow event, the pier of the Chengdu–Kunming Railway Bridge located in Liziyida Gully reported failed,

resulting in 130 people and 146 people reported dead or missing and injured respectively, making it the worst debris flow accident in China's highway history (Yan et al., 2020).

Similarly, Turag-Bhakurta Bridge was a 67 m long bridge constructed in 1995. It experienced two failures; a partial collapse in 1995, which was because of the settlement of the pier due to the 1995 flood, and a complete collapse of the structure because of the reduction in floodwater path during the 1998 flood (Bala et al., 2005). Again, Karnaphuli Bridge was a 920 m long road bridge constructed between 1988 and 1989 using used steel trusses donated by the Dutch government to cross over the Karnaphuli River. The failure was because of a Category V super cyclone on the 29th April 1991, which hit the coastal areas of Bangladesh with up to 225 kmph accompanied by storm surges up to 6m high (Choudhury & Hasnat, 2015).

Mongolia Viaduct was a six-lane single-column-pier viaduct that collapses in the Inner Mongolia Autonomous Region in 2007 because of passage of three overloaded trucks eccentrically on the nearside passing lane resulted in the loss of four lives (Xiong et al., 2017). Similarly, Kings Bridge Melbourne (1962) crosses over a railway, some streets, and the Yarra River in an N-S direction; its collapse occurred on the July 10, 1962 because of overloading beyond the strength limits of both the I-girder and the soil conditions (Choudhury & Hasnat, 2015). Again, I-35W Bridge located in Minnesota was damaged in 2007 which resulted in the loss of about 13 lives and 145 people severely injured (Deng et al., 2015; Feldman, 2010).

Hardinge Railway Bridge is a 1.62 km long steel truss bridge, design and constructed from 1908 to 1915. This Hardinge Railway Bridge crosses over the Padma River between Paksey and Bheramara, Pabna. Two noticeable failure events occurred within its 100 years of service. First was on the 25 September 1933, where the right guide bank was destroyed because of turbulent flow resulting from a flood event (Warrier, 1977; Ghoshal, 2015). The second damaged occurred

during the War of Liberation of Bangladesh in 1971, where one of the 18.3 m steel spans fell off as a result of a direct missile hit, and another one was blown off by explosives placed on the bridge span by the army as a part of war strategy (Ghoshal, 2015).

Materials and Methods

Description of the Study Area

Sebeta – Djibouti Railway line is the only railway line connecting the two countries' cities (Ethiopia and Djibouti). It covers about 30 percent of cultivated land as well as the population of Ethiopia, while about 70 percent population of Djibouti (Mohapatra, 2016). The line has a total length of 752.7 km with double-track for the first 115km from Addis Ababa to Adama, and a single track for the remaining 600km to Djibouti with 21 stations, 61 bridges, 37 frame bridges, and 453 cross culverts along the route (Taju, 2020). Figure 2 is a map of Ethiopia showing the Sebeta - Djibouti Railway Line.

Route and Alignment Location

The Sebeta – Adama Section of Ethio – Djibouti Railway line is about 115 km in length and has about 203 drainage structures in total - 168 slab culverts, 23 frame bridges, and 12 simple supported T-Beam bridges. The slab culverts range from 1.5m to 6.0m top width. However, owing to the limitations such as the DEM resolution, chosen Number of cells to define streams, and the selected number of area square kilometer to define stream, only forty-seven drainage structures in total were captured after the catchment and stream network delineations for further analyses. These structures also comprise 30 slab culverts, 10 simple supported T-Beam, and 7 frame bridges. Figure 3 shows the geographical locations and the structures along the route.

Topographic Description of the Study Area

The case study section of Ethio – Djibouti is within $38^{0}24^{1}0^{11}$E and $9^{0}0^{1}0^{11}$N (West Shewa) and $39^{0}36^{1}0^{11}$E and $8^{0}42^{1}0^{11}$N (East Shewa) in the largest region in terms of landmass (Oromia region) with total length of about 115 km. It is located within Uplands, Upper valley, and Western Highlands of Awash River Basin. Its elevation ranges between 915 – 3550 a.m.s.l (West Shewa being at a higher elevation relative to East Shewa) (Keno, 2020) Figure 3.

In this section, rainfall is very high and it is a cause of flooding which may induce phenomena such as scour, erosion, hydraulic jump, debris impact on bridge foundation (Deng et al., 2015; Witzany et al., 2008; Hong et al., 2012). Again, the predominant geological features are Quaternary, Quaternary Igneous, Tertiary Igneous, and Water (river and lakes). In addition, following the methodological procedure used by (Solihu & Bilewu, 2022), the LULC of the area is majorly built-up areas at Sebeta and Adama while it is mostly Croplands between Bishoftu and Mojo towns with overall accuracy and Kappa Coefficient of about 90.78% and 89% respectively as shown in Figure 4 and Table 2.

Climatic Description of the Study Area

Ethiopia is located in Eastern Africa with its most portion as highland and plateaus. In Ethiopia, temperatures vary from place to place because of huge differences in latitude. Generally, the country has a moderate climate. The rainy season is from June to September while the dry season starts from May to October every year. Again, the hottest months are March, April, and May with approximately 37^{o}C while the coolest months are usually from November to January with approximately 0^{o}C in highland areas. In addition, the heaviest rainfall usually occurs in July and August. These are shown graphically in the forms of maps and bar charts as in Figures 8 – 11, which were developed from the data sourced from both MoWIE and NMAoE.

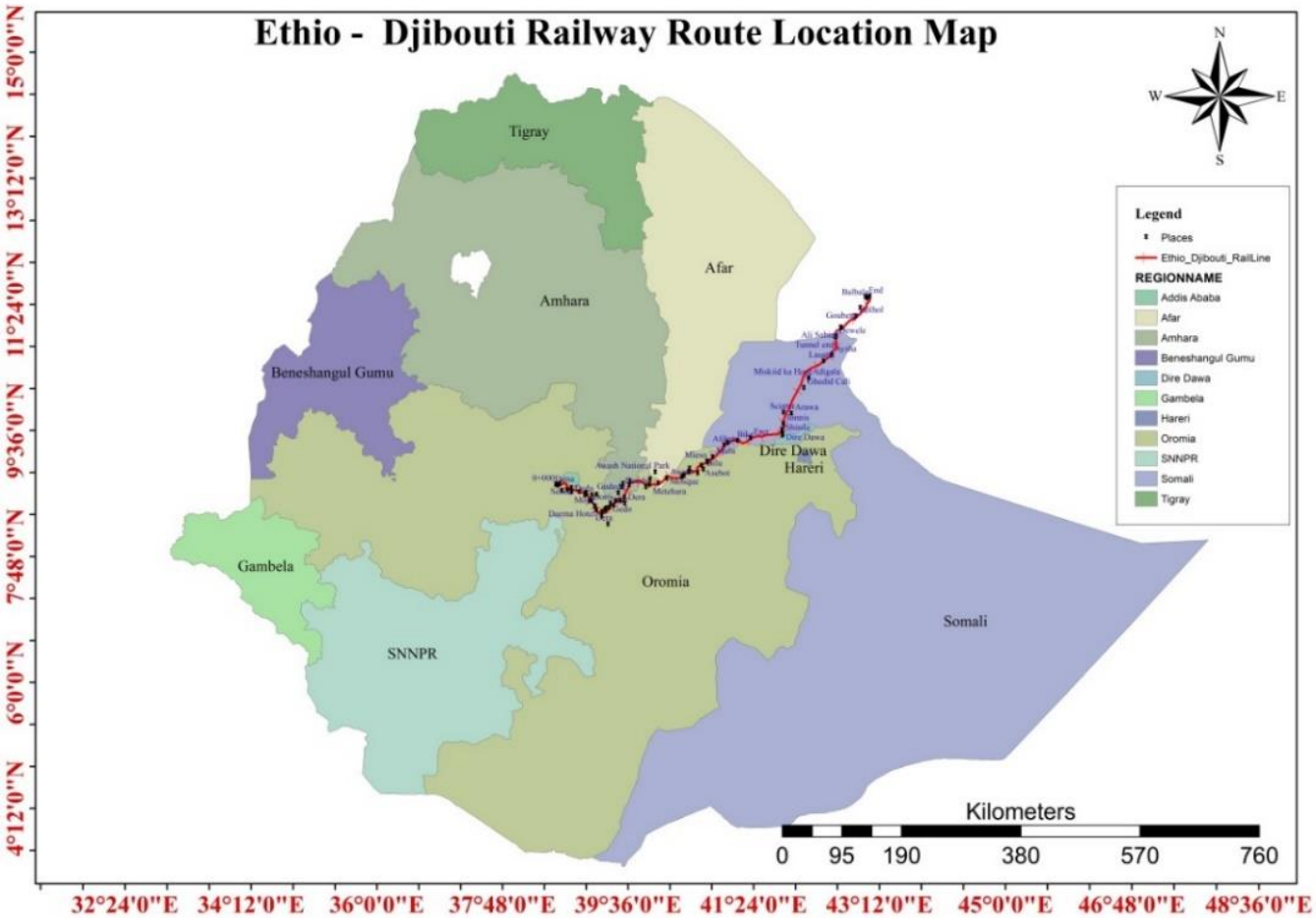


Figure 2: Map of Ethiopia Showing the Ethio - Djibouti Railway Line

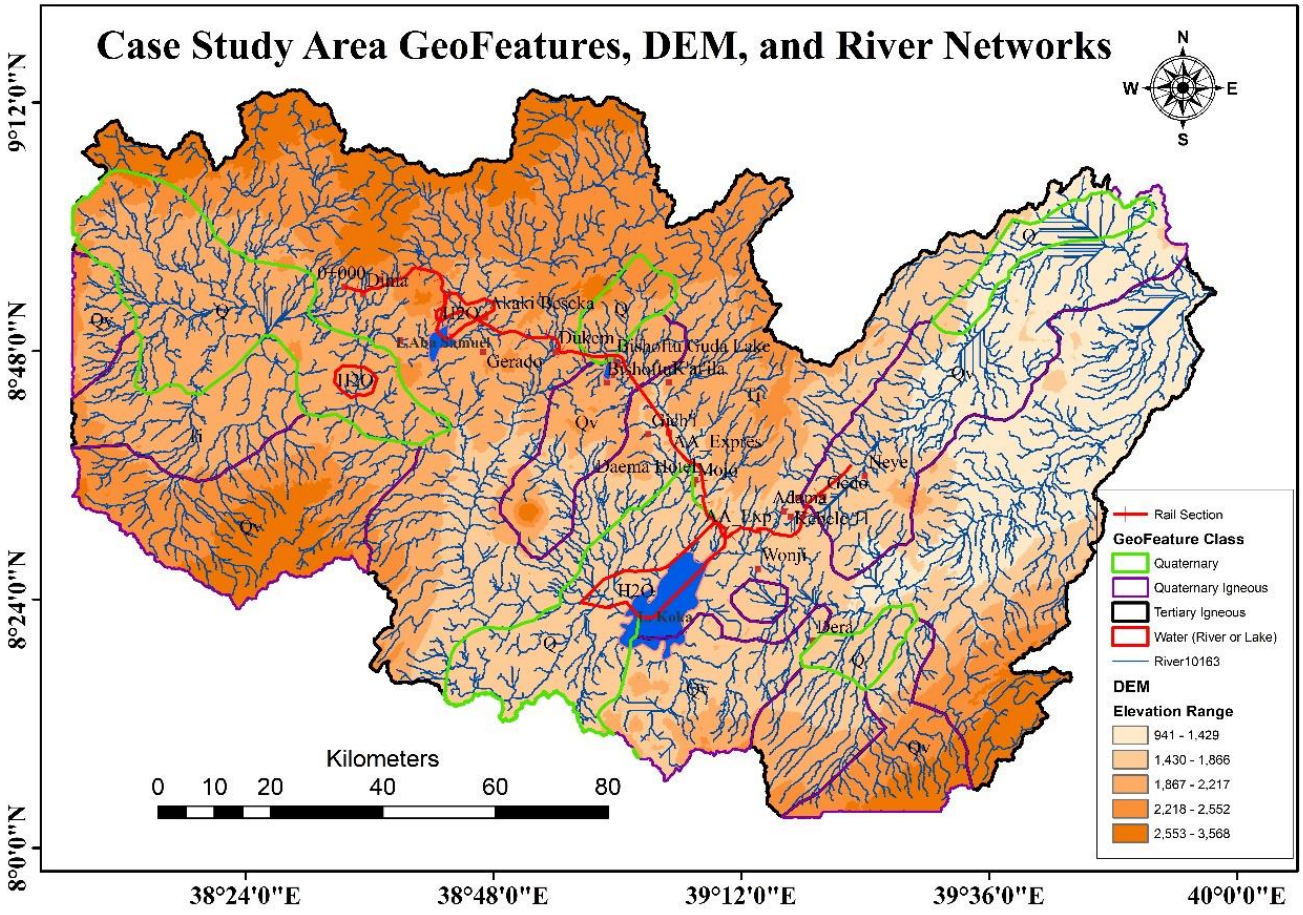


Figure 3: Sebeta - Adama Section Route Location, Geological Features, DEM, and Stream Network

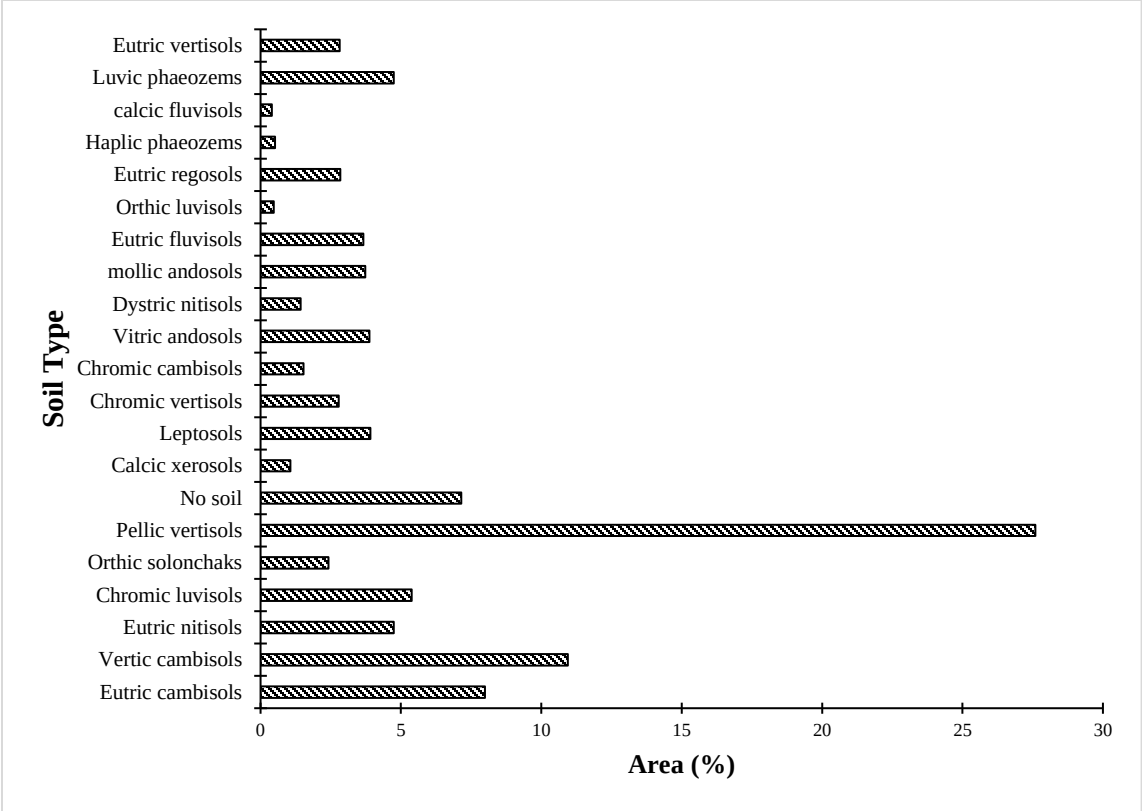


Figure 4: Study Area Soil Texture and their Percentage Area (%)

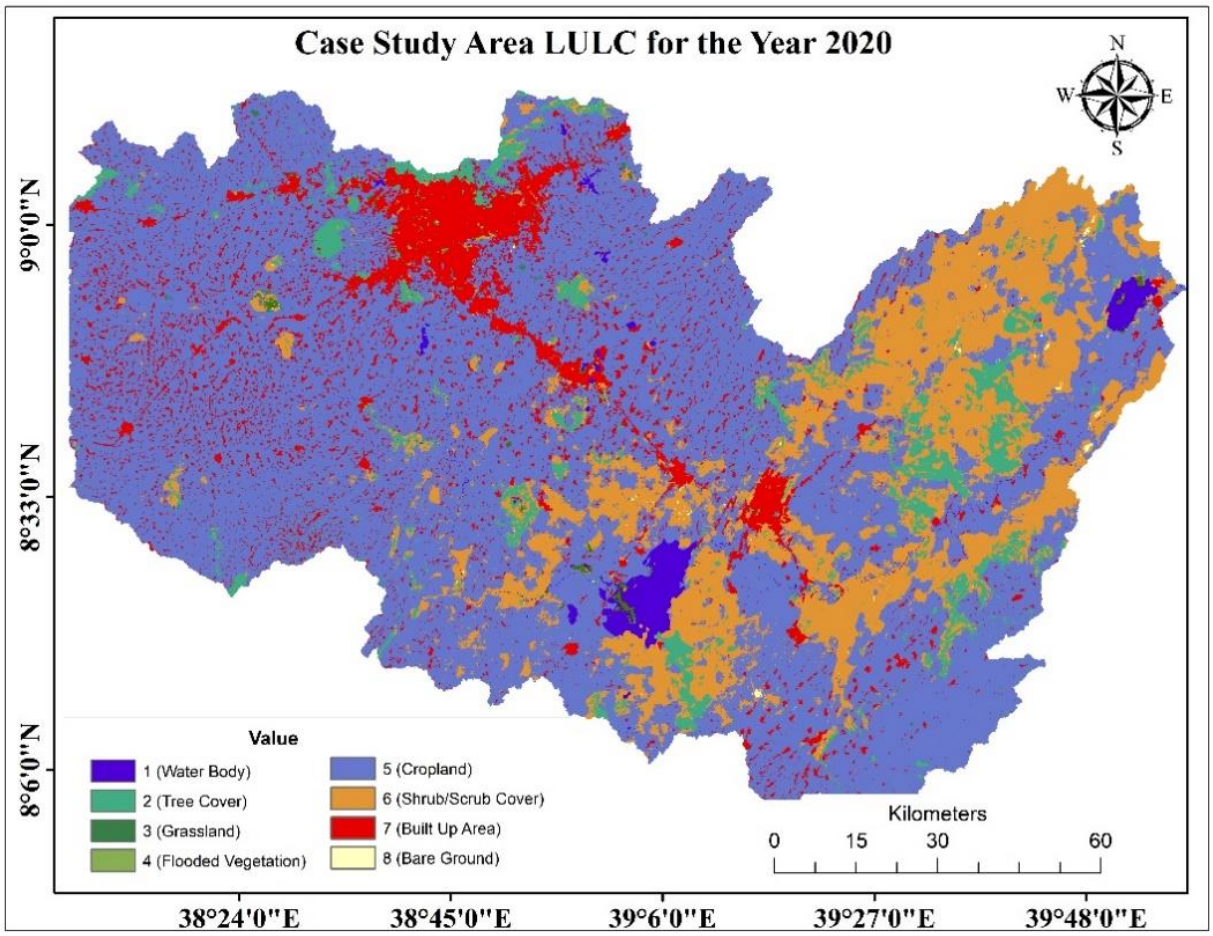


Figure 5: Study Area 2020 LULC Map

From Table 2, the *Overall Accuracy was estimated as 90.97% while the Kappa Coefficient was 89%*. We interpreted this to mean that the classification is excellent and well represents the land use and land cover in the study area.

Table 2: The Year 2020 LandUse LandCover Accuracy Assessment Result using Kappa Coefficient

User's Accuracy	**(%)**	**Producer's Accuracy**	(%)
Bare Areas =	50.0	Bare Areas =	40.0
Built Up Areas =	100.0	Built Up Areas =	80.0
Croplands =	85.0	Croplands =	100.0
Flooded Vegetation =	100.0	Flooded Vegetation =	100.0
Grasslands =	50.0	Grasslands =	83.3
Shrubs Cover Areas =	90.3	Shrubs Cover Areas =	93.3
Tree Cover Areas =	96.3	Tree Cover Areas =	92.9
Water Body =	100.0	Water Body =	100.0

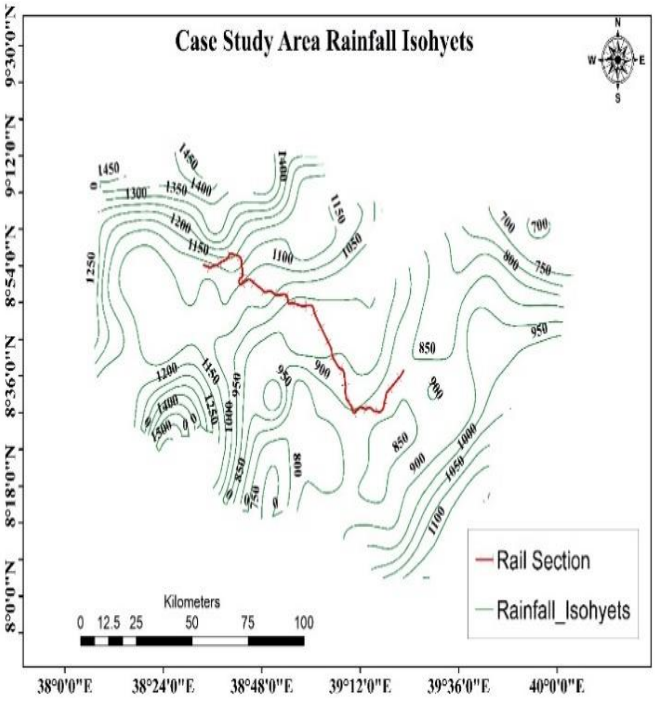


Figure 6: Study Area Rainfall Isohyets

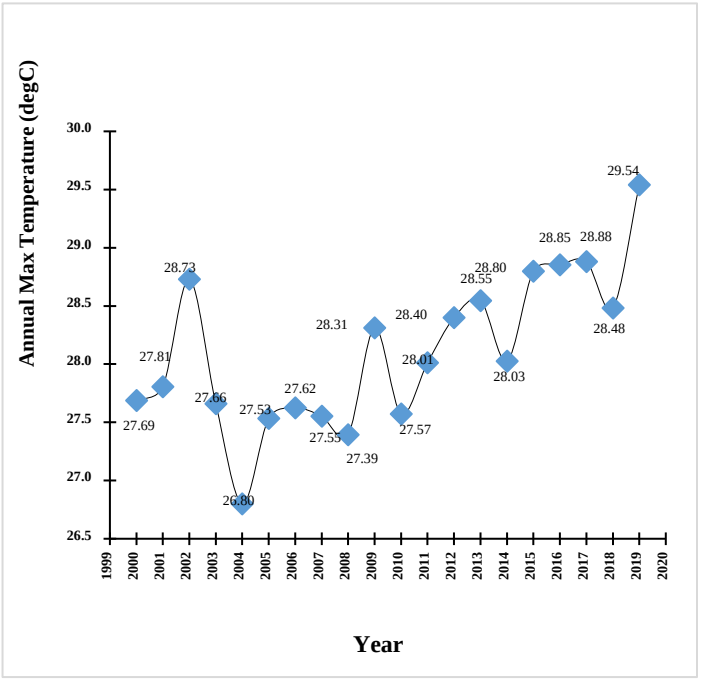


Figure 7: Study Area Annual Average Max. Temperature

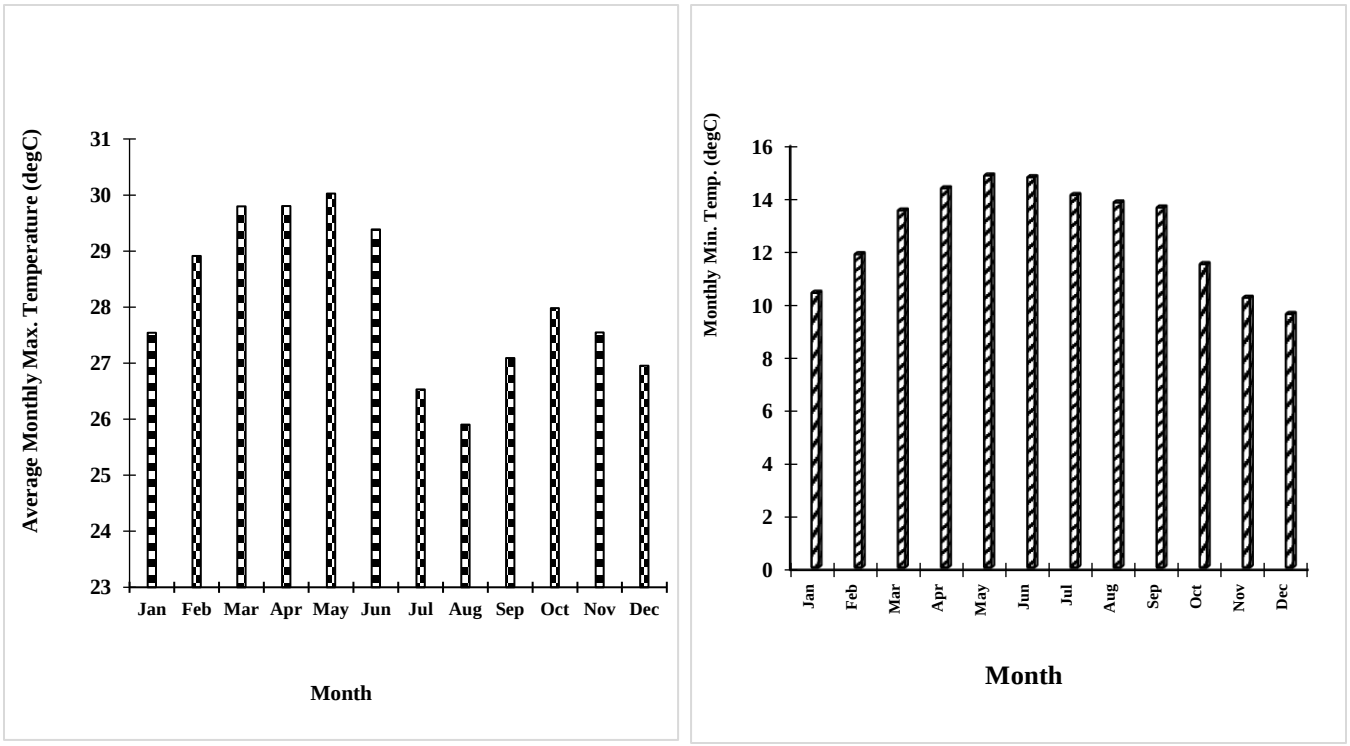


Figure 8: Study Area Monthly Average Max and Min. Temperature (^0C)

Data Collection

Secondary dataset and field observations were used for this study and are classified into three major classes: spatial data and meteorological data. Spatial data (GIS shapefiles), Railroad Alignments and Standards (from Ethiopian Railway Corporation), Meteorological and flow datasets from the relevant agencies in Ethiopia. In addition, some field observations such geographical coordinates and route alignments were carried out to supplement the acquired secondary dataset.

Spatial and Railroad Alignment Data

Spatial Data (GIS shape files), comprising of the Digital Elevation Model (DEM) of high resolution (12.5m), Rivers and lakes, land use data, and Soil Type data, Geographical features, Rainfall-Isohyets, Subbasins, were sourced from the Geographical Information System Department, a unit under the Ministry of Water, Irrigation and Electricity of Ethiopia, located in Addis Ababa. Moreover, the Railroad alignments and standards for the drainage structures (culverts and bridges) within the study area shall be sourced from the Ethiopian Railway Corporation, Addis Ababa, Ethiopia.

Hydrological and Climate Data

Climate data such as rainfall and temperature data for 20 years (2000 – 2019), because there's availability of full data record for these periods for all the ground-based meteorological gauge stations within the uplands and the upper valley of Awash River Subbasins sourced from the National Meteorology Agency of Ethiopia (NMAoE) for the simulation of discharge within the catchment. Also, three hydro-gauge stations within the Awash River Subbasins with full data, which was collected from the Ministry of Water, Irrigation, and Energy (MoWIE). These time-

series datasets were divided into two parts, 2005 – 2010 for the calibration while 2011 - 2014 were used for the validation of the hydrological model.

Data Preparation

Climate and Hydrological Data

Missing Rainfall Estimation & Data Consistency Check

For estimation of data at a station with a similar condition, Linear Regression is the most suitable method. Thus, this study used the linear regression equation to estimate the missing rainfall data by using the station that has the highest correlation coefficient. In addition, simulating the hydrological process in a model, the rainfall data must be checked for consistency. Damaged measuring instruments, measurement errors and geographical paucity of data (data gaps) could cause data inconsistency. Other causes of data inconsistency are changes to instrumentation over time, a change in the measurement site, a change in data collectors, the measurement irregularity, or severe changes in tropical zone climate, precipitation data are frequently incomplete (Wondmagegn, 2020). Thus, double mass curve method was used for correcting the data inconsistencies. Figure 9 shows the original and adjusted double mass curves for Bofa meteorological gauge station.

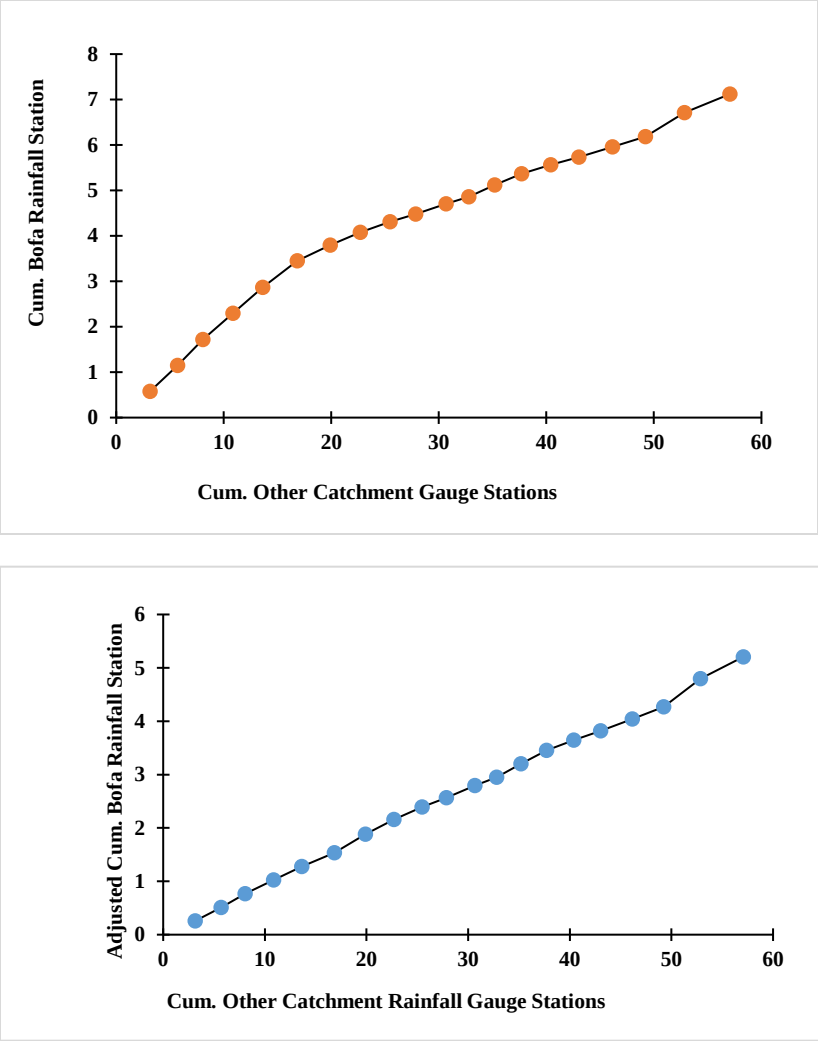


Figure 9: Bofa Original and Adjusted Double Mass Curves

Estimation of Catchment Climate Data and Hydrological Data

There are more than fifteen (15) ground-based meteorology gauge stations within the study area subbasins; however, this study selected only the relevant stations, and the Thiessen Polygon method was used to estimate the catchment climate data as shown in Figure 10. In addition, out of twelve (12) Hydrometric Gauge Stations, only three (3) stations were selected for model calibration and validation because of their full data record availability and connections to the case study. As shown in Figure 11, these gauge stations are enclosed using square boxes.

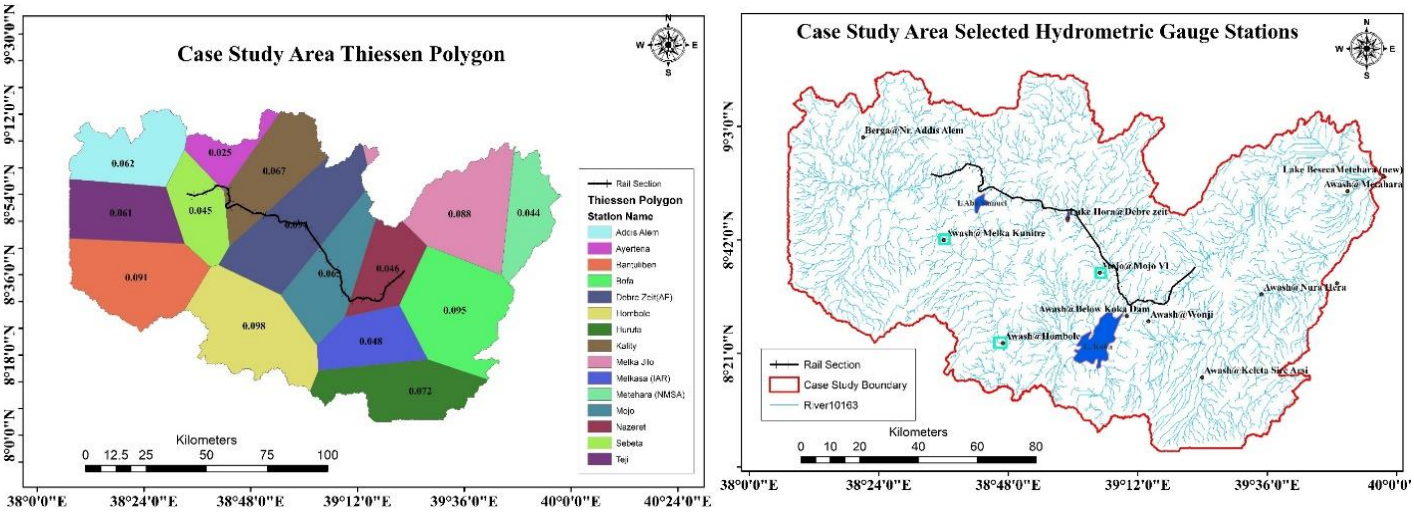


Figure 10: Study Area Thiessen Polygon Map

Criteria for Model Selection

The best and appropriate model selection is prerequisite in any research work. Most often, it is difficult to determine the relative pros and cons of models proposed for operational use. The selection of modeling software is often made on much more realistic grounds. The potential user's familiarity with the techniques employed by the software in addition to the techniques applied by the users' knowledge to produce more results that are realistic is one of the major considerations in model selection (Alaghmand et al., 2012). Following the criteria commonly used by researchers/hydrologist**s** for model selection (Dawit, 2015), the HEC-HMS model was selected to simulate the hydrological processes.

Model Performance Check

The model was calibrated and validated by comparing the simulated flows at the selected HG stations with the observed flows between 2005-2010 and 2011-2014 respectively. The

performance was checked the Nash Sutcliff Efficiency (NSE) (Solihu & Bilewu, 2021; Adegoke et al., 2022), PBIAS, and Coefficient of Determination (r^2) (Solihu & Bilewu, 2021) using Equations 1, 2, and 3 respectively.

$$NSE = 1 - \frac{\sum_{i=1}^{n}(OBS - SIM)^2}{\sum_{i=1}^{n}(OBS - \overline{OBS})\text{^}2} \quad \text{Eq. (1)}$$

$$PBIAS = \left[\frac{SIMV - OBSV}{OBSV}\right] * 100 \quad \text{Eq. (2)}$$

$$r^2 = \left(\frac{\sum_{i=1}^{n}(OBS - \overline{OBS}) * (SIM - \overline{SIM})}{\sqrt{\sum_{i=1}^{n}(OBS - \overline{OBS})\text{^}2 * (SIM - \overline{SIM})\text{^}2}}\right)^2 \quad \text{Eq. (3)}$$

Where;

OBS = Observed values

SIM = Simulated values

V = Volume (m^3)

Drainage Structures Selection Criteria

Employing the model validation, the following criteria were used to select the structures for further considerations:

i. Grouped the drainage points into the numbers of major sub-catchments within the study area i.e. Melka Kuntire, Hombole, Mojo, and others
ii. Determined the daily flow variabilities at each drainage point by calculating their coefficient of variances
iii. Categorized the hydraulic structures at each drainage point into three categories i.e. slab culverts, frame bridges, and simply supported T-beam bridges.

The selection is therefore, based on the hydraulic structures with a large coefficient of variance, and comprises bridges and culverts for further analyses.

Flow Variability Check

The flow variability was checked by calculating the coefficient of variance for the daily flows estimated for each drainage structure. This coefficient of variance was calculated using Equation 4.

$$\mathrm{CoV} = \frac{\mathrm{Stdev}}{\mathrm{Mean}} \qquad \text{Eq. (4)}$$

Where;

CoV = Coefficient of Variance

Mean = Mean of the daily flow

Stdev = Standard deviation of the daily flow

Flood Storm Frequency Analysis

To estimate the peak discharge at the outlets of the selected drainage structures based on the variability check results, this study developed a rainfall and rainfall intensity – duration frequency curves used as a major input data in HEC-HMS to simulate the peak discharges at the selected drainage points.

Peak Annual Rainfall Estimation

The peak daily rainfall magnitudes were selected for each year, which represented the annual peak rainfall values. The result is shown in Table 3.

Table 3: Estimated Annual Peak Rainfall (mm)

Year	Annual Peak Rainfall (mm)	Year	Annual Peak Rainfall (mm)
2000	41.323	2010	40.705
2001	50.677	2011	42.431
2002	52.225	2012	46.055
2003	59.861	2013	42.815
2004	53.601	2014	33.489
2005	48.204	2015	35.279
2006	59.691	2016	73.327
2007	57.433	2017	45.526
2008	57.652	2018	35.239
2009	46.455	2019	32.228

Determination of Goodness-of-fit

The peak annual rainfall magnitudes were subjected to statistical analyses to determine the best probability distribution that best fit the trends in the magnitudes. This research uses EasyFit software, selected about seven (7) different probability distributions while Kolmogorov, Anderson Darling, and Chi-Squared were selected to statistically rank the best distribution as shown in the summary Table 4. Thus, Gen. Extreme Value probability distribution with the probability distribution curve shown in Figure 12 was selected for the estimation of design rainfall magnitudes at different return periods.

Table 4: Summary Table for the Goodness of Fit Used for Ranking Distributions

Goodness of Fit - Summary							
#	Distribution	Kolmogorov Smirnov		Anderson Darling		Chi-Squared	
		Statistic	Rank	Statistic	Rank	Statistic	Rank
3	**Gen. Extreme Value**	**0.08827**	**1**	**0.18473**	**1**	**0.24563**	**4**
2	Chi-Squared (2P)	0.09961	2	0.22379	5	0.34864	6
4	Log-Pearson 3	0.10009	3	0.19583	2	0.21786	3
5	Lognormal	0.10472	4	0.20709	3	0.24886	5
9	Weibull (3P	0.10805	5	0.28385	7	0.17593	1
6	Lognormal (3P)	0.10812	6	0.22348	4	0.20143	2
1	Chi-Squared	0.10837	7	0.25787	6	0.35901	7
8	Weibull	0.1265	8	0.47764	8	0.72413	8
7	Power Function	0.38556	9	4.695	9	8.0001	9

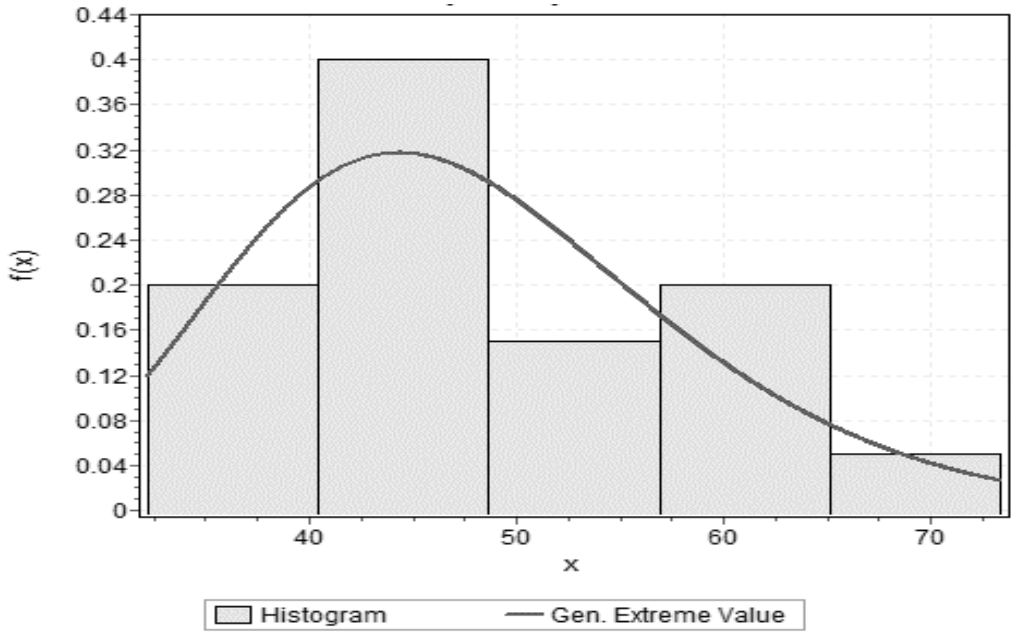


Figure 12: Probability Distribution Curve for Gen. Extreme Value

Results and Discussions

Hydrological Model Setup

The hydrological model (HEC-HMS) was developed in ArcGIS 10.4 using HEC-GeoHMS and Arc Hydro Tools extensions for catchment and river delineation and location of drainage points as shown in Figure 13 following the steps-by-steps processes in the methodological flow chart of this study. In this model, the whole catchment considered is 17,030.00 km^2 in size with a total number of 4 sub-major catchments.

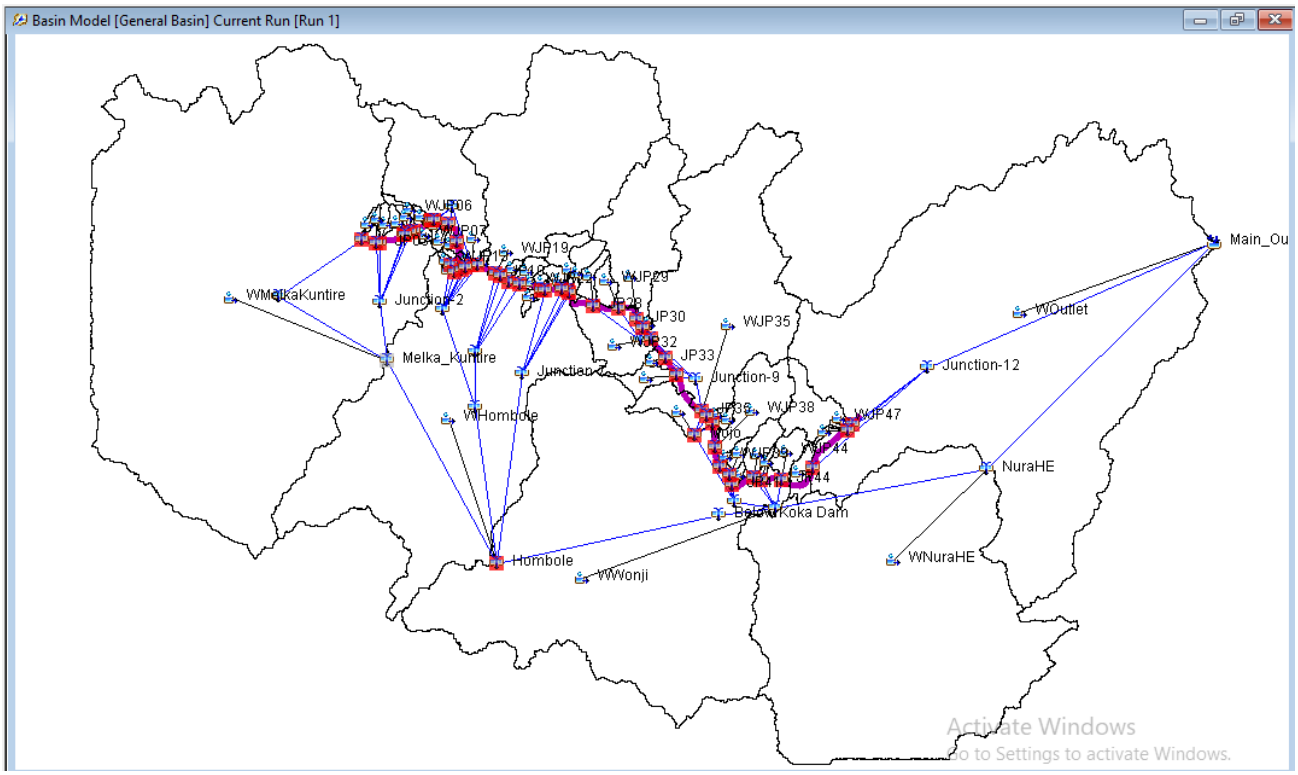


Figure 13: HEC-HMS Model Setup

Catchment Parameters

This study simulated the hydrological processes by selecting the Muskingum method and the Muskingum constant K ranges from 26.11 to 56.55 (hr^{-1}), SCS Runoff Curve Number (85 to 88), and SCS Unit Hydrograph Lag Time (9.07 to 340.93 minutes) as the routing, the loss, and the flow transform methods respectively.

Model Performance Check

The summary of model performance is summarized as shown in Table 5. This indicated that the model performance is within the statistical ranges for surface-runoff simulation.

Table 5: Summary of Model Performance Check Using NSE, PBIAS, and R^2 Statistical Methods

HG Station	Calibration Period	2005 -2010	Validation Period	2011 - 2014
Melka Kuntire HG Station	NSE	0.938	NSE	0.951
	PBIAS %	10.54%	PBIAS %	14.94%
	R^2	0.9994	R^2	0.9979
	Overall: Very Good		Overall: Very Good	
Hombole HG Station	NSE	0.892	NSE	0.938
	PBIAS %	16.36%	PBIAS %	16.28%
	R^2	0.9994	R^2	0.9976
	Overall: Very Good		Overall: Very Good	
Mojo HG Station	NSE	0.942	NSE	0.921
	PBIAS %	6.11%	PBIAS %	12.34%
	R^2	0.917	R^2	0.9617
	Overall: Very Good		Overall: Very Good	

Flow Variability

Since the coefficient of variance is very high at the junction points (0.645 to 1.034) as shown in Tables 6 through 8. It is indicated that there is flow variability at the drainage structures within the selected reach. Group 1, Group 2, and Group 3 indicated all the hydrologic elements found within Melka Kuntire, Hombole, and Mojo with Other catchments respectively, while the drainage structures are labeled JPs.

Table 6: Descriptive Statistics for Group 1

Element	Mean	Std. Dev.	Variance	CoV
JP 01	0.24	0.18	0.03	0.73
JP 02	0.20	0.15	0.02	0.73
JP 03	0.41	0.29	0.09	0.72
JP 04	0.43	0.31	0.10	0.72
JP 05	0.33	0.23	0.06	0.71
JP 06	1.13	0.77	0.60	0.69
JP 07	0.53	0.38	0.14	0.72

Table 7: Descriptive Statistics for Group 2

Element	Mean	Std. Dev.	Variance	CoV	Element	Mean	Std. Dev.	Variance	CoV
JP 08	0.20	0.15	0.021	0.74	JP 18	0.12	0.09	0.008	0.76
JP 09	0.20	0.14	0.020	0.70	JP 19	25.91	18.51	342.583	0.71
JP 10	0.06	0.06	0.004	1.03	JP 20	0.20	0.15	0.022	0.74
JP 11	0.22	0.16	0.026	0.73	JP 21	0.50	0.36	0.131	0.72
JP 12	0.09	0.08	0.006	0.88	JP 22	0.11	0.09	0.007	0.77
JP 13	0.09	0.08	0.006	0.87	JP 23	0.28	0.20	0.041	0.73
JP 14	0.16	0.12	0.014	0.73	JP 24	0.56	0.37	0.140	0.67
JP 15	0.13	0.10	0.009	0.74	JP 25	0.35	0.25	0.062	0.71
JP 16	0.11	0.08	0.007	0.79	JP 26	1.01	0.72	0.523	0.71
JP 17	10.09	7.12	50.692	0.71	JP 27	0.64	0.46	0.210	0.72

Table 8: Descriptive Statistics for Group 3

Element	Mean	Std. Dev.	Variance	CoV	Element	Mean	Std. Dev.	Variance	CoV
JP 28	0.73	0.52	0.27	0.72	JP 38	0.09	0.08	0.01	0.88
JP 29	8.15	5.82	33.92	0.71	JP 39	38.73	27.67	765.81	0.71
JP 30	0.10	0.08	0.01	0.81	JP 40	0.16	0.12	0.01	0.73
JP 31	2.62	1.87	3.51	0.72	JP 41	1.10	0.79	0.62	0.72
JP 32	11.85	7.82	61.10	0.66	JP 42	0.17	0.13	0.02	0.73
JP 33	0.95	0.68	0.46	0.71	JP 43	1.05	0.75	0.57	0.71
JP 34	19.27	13.77	189.59	0.71	JP 44	0.83	0.59	0.35	0.72
JP 35	32.17	20.75	430.60	0.65	JP 45	0.68	0.49	0.24	0.72
JP 36	0.24	0.18	0.03	0.73	JP 46	0.12	0.09	0.01	0.75
JP 37	3.53	2.52	6.35	0.71	JP 47	2.37	1.69	2.87	0.72

Flood Frequency Analysis

The peak flows at the selected drainage structures using the estimated designed rainfall (mm) at different return periods as input data in HEC-HMS, and the peak flows at the drainage structures corresponding to 100 years return period were used for the flood risk assessment.

Design Rainfall Estimation

This study uses the Gen. Extreme Value (GEV) to estimate the design rainfall magnitudes at different return periods for different durations. The rainfall–duration frequency and rainfall intensity–duration frequency tables and curves were developed as presented in Table 9, Figure 14, and Table 10, Figure 15 respectively. The rainfall magnitudes corresponding to 24hrs were used as input in HEC-HMS for estimating the peak flows.

Table 9: Rainfall (mm) Vs Return Periods at Different Durations

Duration (minutes)	Rainfall (mm) vs Return Period							
	2 yrs	5 yrs	10 yrs	25 yrs	50 yrs	100 yrs	200 yrs	500 yrs
5	6.96	8.37	9.31	10.48	11.36	12.23	13.09	14.23
15	10.04	12.07	13.42	15.12	16.38	17.63	18.88	20.53
60	15.94	19.17	21.30	24.00	26.00	27.99	29.97	32.58
120	20.08	24.15	26.84	30.24	32.76	35.27	37.76	41.05
180	22.99	27.64	30.72	34.62	37.51	40.37	43.23	47.00
360	28.97	34.83	38.71	43.62	47.25	50.87	54.46	59.21
720	36.49	43.88	48.77	54.95	59.54	64.09	68.62	74.60
1440	45.98	55.29	61.45	69.23	75.01	80.74	86.46	93.99

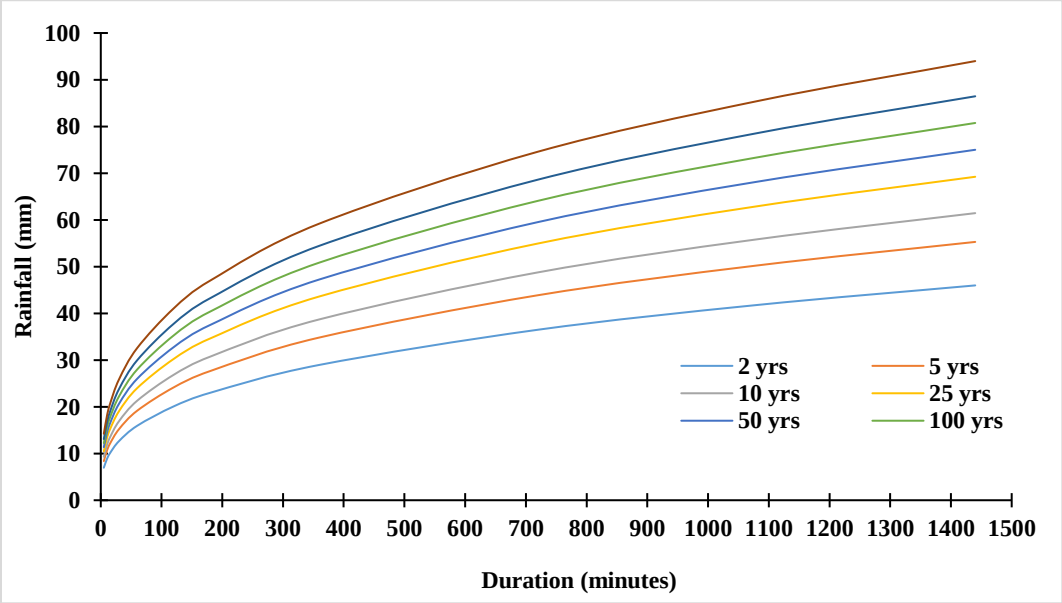


Figure 14: Catchment Rainfall (mm) – Duration Frequency Curve

Table 10: Rainfall Intensity (mm/hr) Vs Return Periods at Different Durations

Duration (Minutes)	Rainfall intensity (mm/hr) vs Return Period							
	2 yrs	5 yrs	10 yrs	25 yrs	50 yrs	100 yrs	200 yrs	500 yrs
5	83.55	100.46	111.66	125.81	136.30	146.72	157.10	170.79
15	40.17	48.30	53.68	60.48	65.53	70.54	75.53	82.11
60	15.94	19.17	21.30	24.00	26.00	27.99	29.97	32.58
120	10.04	12.07	13.42	15.12	16.38	17.63	18.88	20.53
180	7.66	9.21	10.24	11.54	12.50	13.46	14.41	15.67
360	4.83	5.80	6.45	7.27	7.88	8.48	9.08	9.87
720	3.04	3.66	4.06	4.58	4.96	5.34	5.72	6.22
1440	1.92	2.30	2.56	2.88	3.13	3.36	3.60	3.92

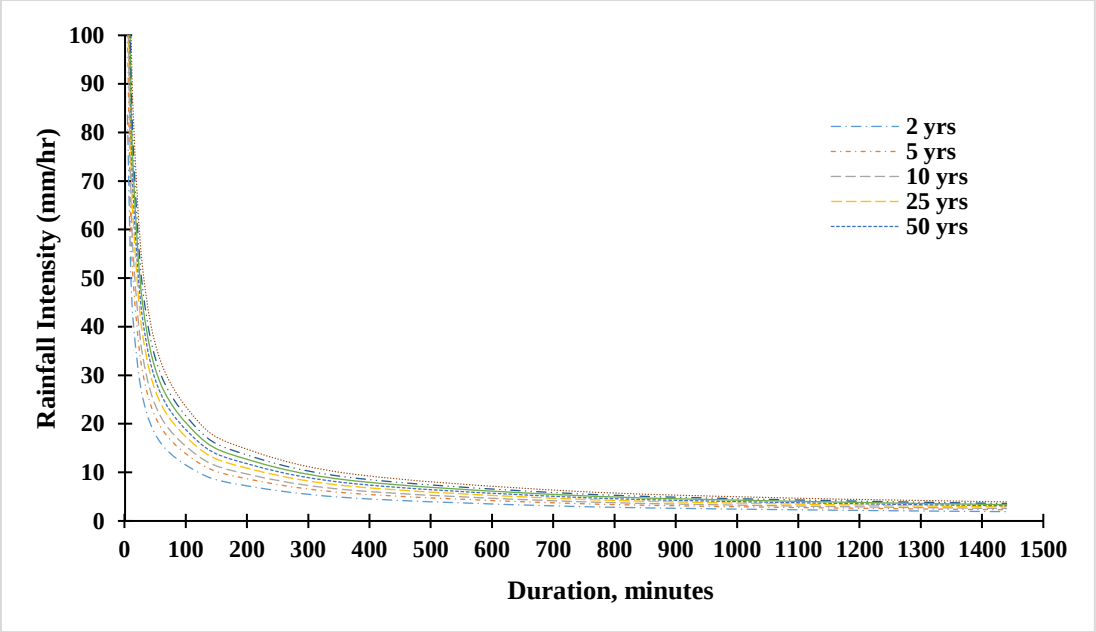


Figure 15: Catchment Rainfall Intensity (mm/hr) – Duration Frequency Curve

Flood Risk Check

This study assessed the drainage structures that are prone to flooding by comparing the estimated peak flows at 100 years return period with the designed flow magnitudes at the same return period extracted from the design documents sourced from ERC. The results of the comparison are presented in Table 12.

Table 12: Comparison between the Estimated and the Design Peak Flows at 100 years Return Periods at the Drainage Locations

Drainage	Q_{100} Design (cms)	Q_{100} Estimated (cms)	Rmrk	Drainage	Q100 Design (cms)	Q100 Estimated (cms)	Rmrk	Drainage	Q100 Design (cms)	Q100 Estimated (cms)	Rmrk
1	47.75	34.20	*	17	106.90	132.04	**	33	8.20	9.20	**
2	65.55	35.60	*	18	28.58	23.30	*	34	NS	46.30	ND
3	128.30	71.30	*	19	98.00	130.72	**	35	535.00	358.50	*
4	57.80	65.60	**	20	NS	33.60	ND	36	27.60	39.20	**
5	71.00	44.10	*	21	NS	68.50	ND	37	34.30	36.04	**
6	63.00	49.20	*	22	3.90	28.40	**	38	13.20	25.40	*
7	63.00	63.70	*	23	24.28	42.20	**	39	45.20	62.10	**
8	13.15	41.90	**	24	23.40	54.80	**	40	8.53	11.01	**
9	12.60	3.30	*	25	186.20	110.96	*	41	21.30	32.98	**
10	7.37	17.20	**	26	174.00	108.50	*	42	178.90	135.90	*
11	NS	46.30	ND	27	10.50	10.30	*	43	46.00	33.00	*
12	18.16	27.00	**	28	159.50	93.50	*	44	NS	115.60	ND
13	21.00	28.20	**	29	109.96	111.98	**	45	13.10	18.46	**
14	48.00	44.50	*	30	273.30	119.50	*	46	18.88	17.90	**
15	54.00	29.50	*	31	8.20	19.82	**	47	5.40	10.15	**
16	52.00	21.70	*	32	141.40	162.87	**				

*** Not prone to flood risk; **prone to flood risk; ND: Not Determined**

As shown in Table 12, about 46% of the drainage structures are prone to flooding at 100 years return period. However, due to insufficient data regarding the probability distribution that was used to estimate the design flows extracted from the document, this study, therefore, could not ascertain the outcome of this flood risk investigation.

Conclusions

The study has developed Rainfall (mm) DF and Rainfall Intensity (mm/hr) – Duration Frequency Curves for the selected catchments, which could also supplement the existing one in the ERA 2013 manual. This study recommends the IDF curve specifically developed for the upland and upper

valley of the Awash River subbasins to complement to the existing IDF curve in ERA 2013 manual for subsequent studies.

This study also concludes that there is flow variability in all the selected drainage structures since the coefficient of variance is very high for all the junction points. The results have revealed that flow variability has effects on flooding and scouring at the drainage structures. In addition, the comparison results between the designed (from the design documents) and the simulated peak flows, Q100 (m3/s), revealed that about 46% of the drainage structure are likely to experience flooding once every 100 years provided that the probability distributions used in this study tallied with that used to estimate the peak flows in the design document.

Therefore, to maintain the socio-economic importance of this line connecting the Ethiopia and Djibouti, the results of this study are so important because drainage structures (bridges and culverts) is one of the major components of a traffic system. Thus, any damage to it could result in partial or complete operation along this line with the potential of causing loss of lives and properties. This could consequently result in an indirect impact on the socio-economy of Ethiopia.

Acknowledgments

The authors acknowledge the National Meteorology Agency of Ethiopia, the Ministry of Water, Irrigation, and Electricity of Ethiopia, and the Ethiopian Railway Corporation for their support during data collection for this study.

Data Availability Statement

All data, models, and code generated or used during the study appear in the submitted article.

Funding

This research did not receive any specific grant from funding agencies in the public, commercial or not-for-profit sectors

Conflict of Interest

The authors declared no conflict of interest in this research paper.

References

Adegoke, H.A., Solihu, H. & Bilewu, S.O. (2022). Analysis of sanitation and waterborne disease occurrence in Ondo State, Nigeria. *Environment, Development and Sustainability*. Pp: 1-19 https://doi.org/10.1007/s10668-022-02558-2

Alaghmand, S., Bin Abdullah, R., Abustan, I., & Eslamian, S. (2012). Comparison between capabilities of HEC-RAS and MIKE11 hydraulic models in river flood risk modeling (a case study of Sungai Kayu Ara River Basin, Malaysia). *Int. J. Hydrol. Sci. Technol*, 2(3), 270-291.

An, M., Lin, W. and Huang, S. (2013). An intelligent railway safety risk assessment support system for railway operation and maintenance analysis, *The Open Transportation Journal*, 7(1), 27-42. doi**:** 10.2174/1874447801307010027

Bala, S. K., Hoque, M. M., & Ahmed, S. M. U. (2005). Failure of a Bridge Due to Flood in Bangladesh-A Case Study. *UAP Journal of Civil and Environmental Engineering*, *1*(1), 38-44.

Choudhury, J. R., & Hasnat, A. (2015). Bridge collapses around the world: Causes and mechanisms. *In IABSE-JSCE Joint Conference on Advances in Bridge Engineering-III*, August 21-22, 2015, Dhaka, Bangladesh. Amin, Okui, Bhuiyan, Ueda (eds.), ISBN: 978-984-33-9313-5

Dawit, S. (2015). Flood risk analysis in Illu Floodplain, Upper Awash River Basin, Ethiopia: A Thesis Submitted to the School of Graduate Studies of Addis Ababa University in Partial Fulfillment of the requirements for the degree of Master of Science in Hydraulic Engin'g. AAU, PG Thesis.

Deng, L., Wang, W., & Yu, Y. (2015). State-of-the-art review on the causes and mechanisms of bridge collapse. *Journal of Performance of Constructed Facilities*, *30*(2), 04015005. DOI: 10.1061/(ASCE)CF.1943-5509.0000731

Dinmohammadi, F., Alkali, B., Shafiee, M., Bérenguer, C., & Labib, A. (2016). Risk evaluation of railway rolling stock failures using FMECA technique: a case study of passenger door system. *Urban Rail Transit*, *2*(3), 128-145. https://doi.org/10.1007/s40864-016-0043-z

Feldman, B. J. (2010). The Collapse of the I-35W Bridge in Minneapolis. *The Physics Teacher*, *48*(8), 541-542. https://doi.org/10.1119/1.3502509

Feng, C. W., Huang, H. Y., & Ju, S. H. (2013). Integrating finite element method with GAs to estimate the scour depth of bridge. *International Journal of Engineering and Technology*, *5*(4), 462. doi: 10.7763/ijet.2013.v5.597

Ghoshal, A. (2015). Saga of Hundred Years of Hardinge Bridge. In A. F. M. S. Amin, Y. Okui, & A. R. Bhuiyan (Eds.). *In IABSE-JSCE Joint Conference on Advances in Bridge Engineering-III*, August 21-22, 2015, Dhaka, Bangladesh. Amin, Okui, Bhuiyan, Ueda (eds.), ISBN: 978-984-33-9313-5

Hofreiter, L., Boc, K., Jangl, S., Lovecek, T., Mach, V., Seidl, M., & Velas, A. (2013). *Protection of critical transport infrastructure objects*. Monograph, 1st edn. EDIS University of Zilina, Zilina.

Hong, J. H., Chiew, Y. M., Lu, J. Y., Lai, J. S., & Lin, Y. B. (2012). Houfeng bridge failure in Taiwan. *Journal of Hydraulic Engineering*, *138*(2), 186-198. DOI: 10.1061/(ASCE)HY.1943-7900.0000430

Keno, A. (2020). Flood Risk Mapping Case Study of Ketar Watershed Ziway-Dugda Woreda, Ethiopia. A Thesis in Hydraulic Engineering Stream. Addis Ababa University Addis Ababa Institute of Technology School of Civil and Environmental Engineering

Lagadec, L. R., Moulin, L., Braud, I., Chazelle, B., & Breil, P. (2018). A surface runoff mapping method for optimizing risk assessment on railways. *Safety science*, *110*, 253-267. https://doi.org/10.1016/j.ssci.2018.05.014

Liu, K., Hou, K., Fei, Z., Shi, R., & Wang, S. (2020). Field test and numerical analysis of in-service railway bridge. *Advances in Materials Science and Engineering*, Vol. 2020. https://doi.org/10.1155/2020/9621591

Mohapatra, D. R. (2017). An economic analysis of Djibouti-Ethiopia railway project. Economic and Financial Analysis of Infrastructure Projects: An Edited Volume, *European Academic Research* 3(10), 11376- 11400.

Sañudo, R., Miranda, M., García, C., & García-Sanchez, D. (2019). Drainage in railways. *Construction and Building Materials*, *210:* 391-412. https://doi.org/10.1016/j.conbuildmat.2019.03.104

Sekasi, J., & Solihu, H. (2021). Safety and risk analysis at railway crossings of north-south Addis Ababa light rail. *Smart and Resilient Transport*. 3(3), 266-282, https://doi.org/10.1108/SRT-08-2021-0007

Solihu H. & Bilewu S. O. (2022). Assessment of anthropogenic activities impacts on the water quality of Asa River: A case study of Amilengbe area, Ilorin, Kwara state, Nigeria. *Environmental Challenges*, 7, 100473. https://doi.org/10.1016/j.envc.2022.100473

Solihu H. & Bilewu S. O. (2021). Availability, coverage, and access to the potable water supply in Oyo State Nigeria. *Environmental Challenges*, 5(C), 10033. https://doi.org/10.1016/j.envc.2021.100335

Yan, S., He, S., Deng, Y., Liu, W., Wang, D., & Shen, F. (2020). A reliability-based approach for the impact vulnerability assessment of bridge piers subjected to debris flows. *Engineering Geology*, *269*, 105567. https://doi.org/10.1016/j.enggeo.2020.105567

Taju, A. (2020). Ethio-Djibouti Railway Line Modernization Project. Ethiopia: Pandit Deendayal Petroleum University, School of Technology.

Vičan, J., Gocál, J., Odrobiňák, J., & Koteš, P. (2016). Existing steel railway bridges evaluation. *Civil and Environmental Engineering*, *12*(2), 103-110. DOI: 10.1515/cee-2016-0014

Wardhana, K., & Hadipriono, F. C. (2003). Analysis of recent bridge failures in the United States. *Journal of performance of constructed facilities*, *17*(3), 144-150.

Warrier, G. P. (1977). Restoration of Hardinge Bridge in Bangladesh. *Proceedings of the Institution of Civil Engineers*, *62*(3), 399-418. https://doi.org/10.1680/iicep.1977.3109

Witzany, J., Cejka, T., & Zigler, R. (2008). Failure resistance of historic stone bridge structure of Charles Bridge. II: Susceptibility to floods. *Journal of performance of constructed facilities*, *22*(2), 83-91. https://doi.org/10.1061/(ASCE)0887-3828(2008)22:2(83)

Wondmagegn, T., & Mengistou, S. (2020). Effects of anthropogenic activities on macroinvertebrate assemblages in the littoral zone of Lake Hawassa, a tropical Rift Valley Lake in Ethiopia. *Lakes & Reservoirs: Research & Management*, *25*(1), 61-71. https://doi.org/10.1111/lre.12303

Xiong, W., Cai, C. S., Kong, B., & Ye, J. (2017). Overturning-collapse modeling and safety assessment for bridges supported by single-column piers. *Journal of Bridge Engineering*, *22*(11), 04017084. https://doi.org/10.1061/(ASCE)BE.1943-5592.0001133